Pilot Study on Vascular Intervention Training based on Blood Flow Effected Guidewire Simulation

Jiayin. Cai, Hongzhi. Xie*, Shuyang. Zhang, and Lixu. Gu*, *Senior Member, IEEE*

***Abstract*—A decent guidewire behavior simulation is vital to the virtual vascular intervention training. The influence of blood flow has rarely been taken into consideration in former works of guidewire simulation. This paper addresses the problem by integrating blood flow analysis and proposes a novel guidewire simulation model.**

The blood flow distribution inside arterial vasculature is computed by separating the vascular model into discrete cylindrical vessels and modeling the flow in each vessel with the Poiseuille Law. The blood flow computation is then integrated into a Kirchhoff rods model. The simulation could be run in real time with hardware acceleration at least 30 fps. To validate the result, an experiment environment with a 3D printed vascular phantom and an electromagnetic tracking(EMT) system was set up with clinical-used guidewire sensors applied in phantom to trace its motion as the standard for comparison.

Experiment results reveal that the shown blood flow effected model presents better physical credibility with a lower and more stable root-mean-square(RMS) at 2.14mm ± 1.24mm, better than the Kirchhoff model of 4.81mm±3.80mm.

I. Introduction

Percutaneous Coronary Intervention (PCI) is an effective procedure used to treat coronary heart disease with the advantage of smaller incisions, less blood loss, decreased pain and quicker recovery [1]. In this procedure, surgeons need to manipulate a guidewire within a three-dimensional (3D) field, while viewing its position on a two-dimensional screen [2]. It is a big challenge to establish a safe and low-cost training environment for inexperienced medical students. Traditional options including synthetic phantoms, animals and human cadaver do help but with limitation [3][4]. The virtual reality technology shows a better way with a VR-based simulation system due to its more realistic sights, higher flexibility, and easier training assessment [3]. Studies proved that training using virtual reality simulation can improve inexperienced surgeons' intervention skills [2][4][5] effectively.

Guidewire simulation is the key to the virtual vascular intervention simulation system. Previously a real-time finite element model with an optimization strategy based on substructure decomposition [6] made it possible to represent the complex behavior of wire-like structure, following with an improved method computing the whole stiffness matrix with its band structure [7]. Elastic rod model is another option. Based on the Cosserat theory of elastic rods, Teschner et al. [8] and Duratti et al. [9] implemented their simulation with better performance than the mass spring model [10][11]. Bergou et al. [12] proposed their Kirchhoff rods model, based on which Tang et al [13] and Luo et al. [14] both built their simulation systems. However, none of the existing work took into account the force of blood on guidewire.

On the other hand, blood flow analysis and simulation are a popular topic among many other researchers. Alemder [15] presented his hydrodynamic model of human arterial blood flow. Based on Poiseuille Law and the Advection-Diffusion Model from the Navier–Stokes equations, Wu et al. [16] computed the blood flow in carotid artery and simulated the propagation of contrast agent. With a similar approach, Zhu et al. [17] built a sketch-based dynamic illustration system for fluids, which was both easy and flexible for users to illustrate fluid systems. Boisvert et al. [18] integrated blood circulation and bleeding model into computerized surgical simulation system by modeling the vessels as a graph and calculating the blood pressures and flows in real time.

This paper, encouraged by Luo's [14] guidewire simulation using the Kirchhoff elastic rod method, sought to integrate blood flow computation to build a novel model. Most former researchers only evaluated their simulation by visual effects To better validate the result of the model that is being proposed, an electromagnetic tracking(EMT) system is introduced to record guidewire track accurately, allowing the proposed virtual guidewire to be compared with the real tracked guidewire in a 3D printed vascular phantom.

II. Real-Time Blood Flow Computation

A. Flow Model

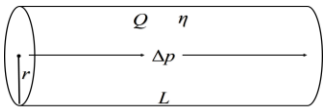

Figure 1. A cylindrical pipe-like vessel

$$Q = \frac{\Delta p}{R} \; with \; R = \frac{8\eta L}{\pi r^4} \tag{1}$$

As Fig.1 shows, the flow model in a small cylindrical vessel with flow rate Q, pressure drop Δp, blood viscosity η, vessel radius r and vessel length L, could be described with an equation called Poiseuille Law calculated from the Navier-Stokes equation as (1) [16].

*Research partially supported by the Chinese 863 National Research Fund and Chinese National Key Research and Development Program

Jiayin. Cai is with the School of Biomedical Engineering, Shanghai Jiao Tong University, Shanghai, China.

Hongzhi. Xie, corresponding author, is with Department of Cardiology, Peking Union Medical College Hospital, Peking 100005, China. (e-mail: drxiehz@163.com).

Shuyang. Zhang, is with Department of Cardiology, Peking Union Medical College Hospital, Peking 100005, China

Lixu. Gu, corresponding author, is with the School of Biomedical Engineering, Shanghai Jiao Tong University, Shanghai, China. (e-mail: gulixu@sjtu.edu.cn).

B. Blood Flow Computation in Vascular Structure

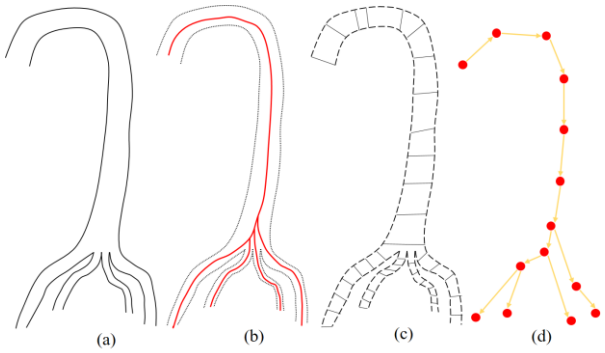

Figure 2. Discretization of vascular model. (a) Original model. (b) Centerline. (c) Discrete model. (d) Abstract model as a directed graph

The simulation in this paper focuses on guidewire moving inside the main artery. As is shown in Fig.2, the original vascular model (a) generated from medical image data could be divided into cylindrical pipes (c) based on centerline (b). Based on the centerline, the continuous vascular structure is separated into cylindrical vessels, the combination of which is an approximation of original structure. The blood flow in each cylindrical vessel thus becomes appropriate for Poiseuille Law modeling as (1).

The separate vessels in the discrete vascular structure are then connected and can be represented as a directed graph [16] $G(N_n, N_e)$, with N_n nodes and N_e edges (Fig.2d). Each node stands for a separate point and each edge for a cylindrical vessel described as a node-edge adjacency matrix A as (2), which has N_n rows and N_e columns.

$$A_{i,j} = \begin{cases} 1 & if\ edge\ j\ starts\ from\ node\ i \\ -1 & if\ edge\ j\ end\ in\ node\ i \\ 0 & otherwise \end{cases} \quad (2)$$

Except the start and leaf nodes, the blood entering and leaving each node is always at the same level, expressed as (3).

$$AQ = 0 \quad (3)$$

For all of the edges in the graph, the Poiseuille Law could be represented in matrix form as (4)

$$CQ = \Delta P \quad (4)$$

C is a diagonal matrix of $\begin{pmatrix} R_1 & \cdots & 0 \\ \vdots & \ddots & \vdots \\ 0 & \cdots & R_{n_e} \end{pmatrix}$ and ΔP is a vector containing the pressure drop of all the edges.

An external periodical time-varying pressure source is added to the root node of the graph as the source of blood flow. The pressure source could be modeled like (5) as a sinusoidal function[18] that varies with time changing between systolic pressure P_1 and diastolic pressure P_2.

$$p_{source}(t) = \frac{P_1 - P_2}{2}\sin(\omega t) + \frac{P_1 + P_2}{2} \quad (5)$$

The blood flow in the whole vascular structure could be developed by combining (1) to (5).

$$\begin{pmatrix} A & 0 \\ C & A^T \end{pmatrix}\begin{pmatrix} Q \\ P \end{pmatrix} = \begin{pmatrix} 0 \\ P_{source}(t) \end{pmatrix} \quad (6)$$

In (6), Q denotes the vector containing the flow rate in each cylindrical vessel, P refers to the vector of pressure value in each node of separate vascular model and $P_{source}(t)$ is deduced from (5) as pressure source.

The equation could be solved explicitly as shown in Equation (7).

$$\begin{pmatrix} Q \\ P \end{pmatrix} = K^{-1}\begin{pmatrix} 0 \\ p_{source}(t) \end{pmatrix}\ with\ K = \begin{pmatrix} A & 0 \\ C & A^T \end{pmatrix} \quad (7)$$

K^{-1} could be precomputed, which leads to less variability on time and less cost on hardware resources during the simulation, and permits real-time computation rates even in a complex structure.

C. Blood Flow Effected Guidewire Simulation

To take blood flow into consideration, each mass point of the simulated guidewire needs to be located in the separate vascular model. The mass points are presented as $m_{1\sim n}$ and the vessels $V_{1\sim n}$. Checking the relative position of each m_i with each V_i could never be wrong. However, it can be dramatically slowed down due to its quadratic complexity. Our strategy is based on the fact that the neighbor mass points usually stay in roughly the same or neighbor vessels. Therefore, it is only necessary to search each vessel from V_1 to V_n for the first mass point m_1 and find out the relative vessel $V_{1'}$. For other points m_i, it is only needed to search the vessels $V_{(i-1)'\pm a}$, which is only a small neighborhood with the length $2a$ that mass point m_{i-1} locates in.

After we located each mass point m_i in a vessel $V_{i'}$, we can define the influence of the blood flow on each mass point. From the vessel flow rate Q and the pressure drops ΔP computed by the vascular flow model mentioned previously, the laminar flow velocity along the axial direction of each vessel is modeled as (8):

$$u(x,d) = \frac{1}{4\eta}\frac{\Delta P}{x}(r^2 - d^2) = \frac{2}{\pi r^2}Q\left(1 - \frac{d^2}{r^2}\right) \quad (8)$$

which indicates the laminar flow velocity at any position in a vessel varying with the radical direction distance d and the axial direction distance x [16].

The flow velocity on every mass point could be integrated into Luo's [14] Kirchhoff model. The dynamic iteration of original Kirchhoff guidewire model is expressed in (9) [14], where x_t and v_t are the location and velocity at time t with the variation of locations (Δx) and velocity (Δv) in time step Δt. M is a diagonal mass matrix associated with mass point positions and $\partial f/\partial x$, $\partial f/\partial v$ are the Jacobian matrices of the force with respect to locations and velocities. With the flow velocity u computed from (8) being an additional item demonstrated in (10), the guide wire simulation is now under the influence of blood flow.

$$\begin{cases} \begin{bmatrix} \Delta x \\ \Delta v \end{bmatrix} = \Delta t \begin{bmatrix} v_t + \Delta v \\ M^{-1}f(x_t + \Delta x, v_t + \Delta v) \end{bmatrix} \\ f(x_t + \Delta x, v_t + \Delta v) = f_t + \frac{\partial f}{\partial x}\Delta x + \frac{\partial f}{\partial x}\Delta v \end{cases} \quad (9)$$

$$\begin{bmatrix} \Delta x \\ \Delta v \end{bmatrix} = \Delta t \begin{bmatrix} v_t + \Delta v \\ M^{-1}f(x_t + \Delta x, v_t + \Delta v) \end{bmatrix} + \begin{bmatrix} 0 \\ u \end{bmatrix} \quad (10)$$

III. Experiments and Evaluation

The simulation system was developed and tested on a PC with Intel® Xeon® E3-1230 CPU, 4G memory and an NVidia GeForce GTX 760 GPU. The model was tested in main artery corresponding to one of the PCI procedures that delivering the guidewire to the mouth of coronary artery. The guidewire simulated is a "J" tipped 0.035 wire which is commonly used in the procedure. The blood flow was computed first and the result was rendered visually. The simulated guidewire was compared with both previous blood flow thoughtless model and the real guidewire with the help of the EMT system.

A. Flow Computation Result

The vascular model was the main artery generated from a patient's CT scan, segmented by a semiautomatic algorithm [19] and centerline extracted with the VMTK library [20]. The discrete vascular structure including 2477 vessels was modeled as a directed graph with 2478 nodes and 2488 edges. It costs about 10 milliseconds per frame to compute the distribution of blood pressure in the vascular model with the Intel MKL library.

The computation result is demonstrated in the Fig.3 (a). The Fig.3 (b) shows the relationship of pressure values and the vessel radius. The pressure decreases significantly when the vessel radius becomes smaller, which is identical with what the Poiseuille Law has indicated.

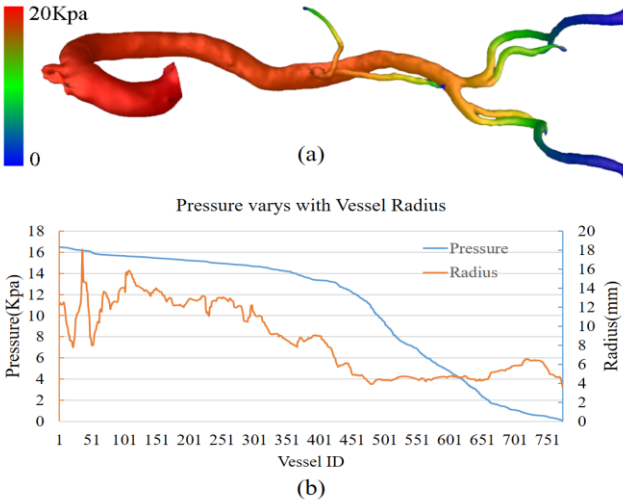

Figure 3. (a)Pressure distribution. (b)Pressure varies with vessel radius

B. Comparison of Simulating guidewire with/without blood influence

We exert a simulated intervention by driving the two simulated guidewires into vascular model by a constant force with and without blood influence simultaneously. In Fig.4, four snapshots captured during the process, show that the motion shape of guidewire under blood flow influence (green) is more bended and closer to the vessel wall when it stays straight without blood pressure (white).

C. Phantom experiment

A vascular phantom was made with tangoplus and veroclear hybrid materials at 4 mm thickness based on the model in simulated environment by an Object500 Connex3

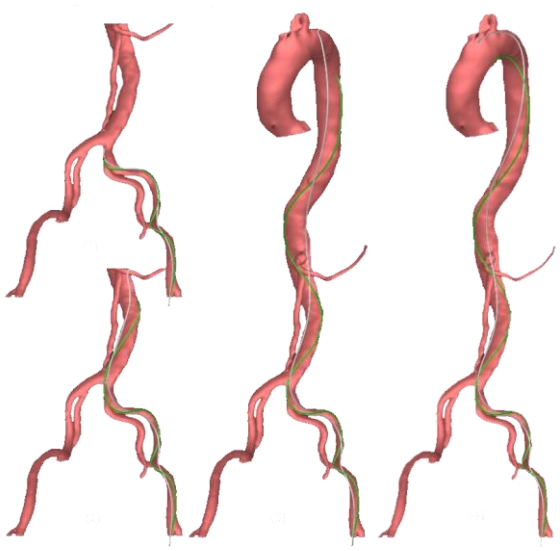

Figure 4. Four snapshots of simulating guidewires with (Green) and without (White) blood force influence

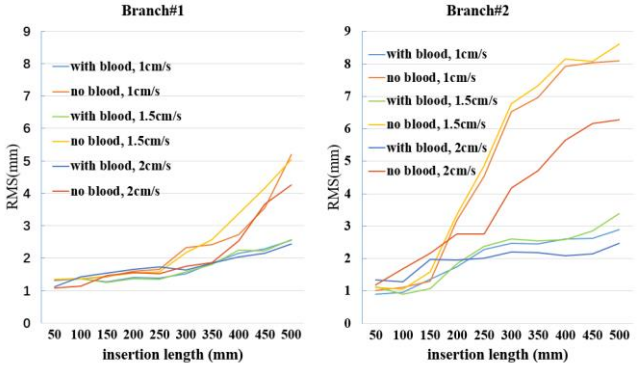

Figure 5. Comparison of the virtual and EMT recorded track of guidewire inserted through branch#1 and branch#2 at different speeds.

3D-printing machine from Stratasys Company. For coordinate transformation, 4 additional landmarks were attached to the phantom. The phantom was placed in a transparent water tank filled with 10% glycerol water and aside by an EM field generator. An optical motion detector was used to synchronize the movement of real guidewire in phantom and virtual guidewire. Because of the hardware limit, a constant external water source was generated to simulate the flow pressure source from the heartbeat with the same pressure source set in simulation model. An EMERALD Guidewire 0.035 from Cordis Corporation, with 3 NDI Aurora 610058 5DOF magnetic sensors binded to the tip was inserted into the phantom while the NDI Aurora EMT system tracked the motion. The guidewire was inserted into the phantom through different branches at different speeds.

The physical guidewire tip trace recorded through EMT system could be regarded as the truth for evaluating simulated tip traces. The result was measured with the root-mean-square (RMS) distance between the two traces as (11).

$$RMS = \left(\frac{1}{n}\sum_{1}^{n}(X_i - Y_i)^2\right)^{1/2} \quad (11)$$

Where X denotes the n simulated track points and Y denotes the reference positions of physical track correspondingly.

The quantitative comparison of the real track and virtual track is recorded in Fig.5, showing the experiment results of the guidewire inserted through branch#1 and branch#2 at 3 different speeds. Fig.5 shows the RMS value changes as guidewire insertion length increases. The RMS of both simulated guidewire traces is small at the beginning, since the blood flow pressure is in a low level in those areas due to small vessel radius and long distance from the pressure source (heart). However, the blood flow affects dramatically as the guidewire gets closer to the pressure source. The blood flow influenced guidewire presents a significant improvement with a lower and more stable RMS of 2.14mm±1.24mm, which is less than half of the simulated guidewire without blood flow influence at 4.81mm±3.80mm.

D. Efficiency Evaluation

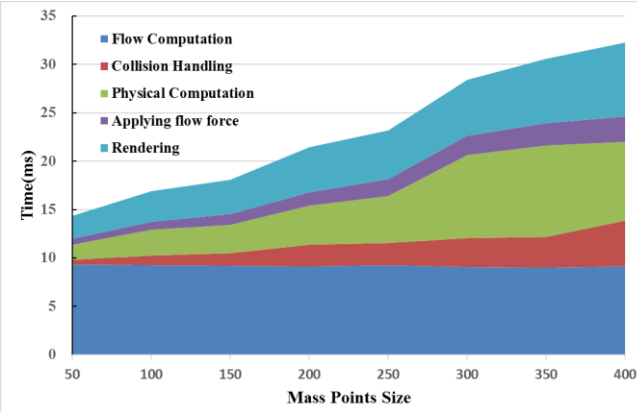

Figure 6. Efficiency of each simulating step

It is demanded to run the simulation in real time. Fig.6 show the summary of the efficiency, including time cost of flow computation, physical computation, collision handling, applying flow force and rendering. It almost costs constant time at about 9ms for flow computation in each frame. Other parts of the computation are of linear complexity with respect to the size of mass point size. The whole simulating procedure could run in real time at 30 fps.

IV. Discussion and Conclusion

This paper presents a more realistic simulated guidewire model by integrating the blood flow analysis into a previous Kirchhoff guidewire simulation model [14]. The simulation could be performed in real time with the help of hardware acceleration and the quantitative validation with EMT system indicates a high level of physical fidelity.

The simulation result received positive comments from doctors due to better physical fidelity than the existing simulator. They confirmed that the improving guidewire simulation would be useful in helping trainees improve their intervention skills.

The flow model is based on an axially oriented laminar flow model currently, which is not perfect that it neglects other factors such as turbulent flow, the systole and diastole influence on flow patterns, non-Newtonian fluid behavior and the elasticity of artery wall. The pressure waveform used right now also does not include the higher frequency information found physiologically. The model could be extended to pulsatile flow in future work, with the elasticity effects taken into consideration.

Acknowledgment

This research is partially supported by the National Key research and development program (2016YFC0106200), and 863 national research fund (2015AA043203) as well as the Chinese NSFC research fund (61190120, 61190124 and 61271318).

References

[1] Y. Fu, H. Liu, W. Huang, S. Wang, and Z. Liang, "Steerable catheters in minimally invasive vascular surgery," *Int. J. Med. Robot. Comput. Assist. Surg.*, vol. 5, no. 4, pp. 381–391, 2009.

[2] R. Aggarwal, S. a. Black, J. R. Hance, a. Darzi, and N. J. W. Cheshire, "Virtual Reality Simulation Training can Improve Inexperienced Surgeons' Endovascular Skills," *Eur. J. Vasc. Endovasc. Surg.*, vol. 31, no. 6, pp. 588–593, 2006.

[3] S. K. Neequaye, R. Aggarwal, I. Van Herzeele, A. Darzi, and N. J. Cheshire, "Endovascular skills training and assessment," *J. Vasc. Surg.*, vol. 46, no. 5, pp. 1055–1064, 2007.

[4] K. Ahmed, A. N. Keeling, M. Fakhry, H. Ashrafian, R. Aggarwal, P. a. Naughton, A. Darzi, N. Cheshire, T. Athanasiou, and M. Hamady, "Role of Virtual Reality Simulation in Teaching and Assessing Technical Skills in Endovascular Intervention," *J. Vasc. Interv. Radiol.*, vol. 21, no. 1, pp. 55–66, 2010.

[5] D. L. Dawson, J. Meyer, E. S. Lee, and W. C. Pevec, "Training with simulation improves residents' endovascular procedure skills," J. Vasc. Surg., vol. 45, no. 1, pp. 149–154, 2007.

[6] S. Cotin, C. Duriez, J. Lenoir, P. Neumann, and S. Dawson, "New approaches to catheter navigation for interventional radiology simulation," Med. Image Comput. Comput. Assist. Interv., vol. 11, no. October 2005, pp. 534–542, 2005.

[7] J. Dequidt, M. Marchal, C. Duriez, E. Kerien, and S. Cotin, "Interactive simulation of embolization coils: Modeling and experimental validation," Lect. Notes Comput. Sci. (including Subser. Lect. Notes Artif. Intell. Lect. Notes Bioinformatics), vol. 5241 LNCS, no. PART 1, pp. 695–702, 2008.

[8] M. Teschner, "C O R D E : Cosserat Rod Elements for the Dynamic Simulation of One-Dimensional Elastic Objects," vol. 1, 2007.

[9] L. Duratti, F. Wang, E. Samur, and H. Bleuler, "A real-time simulator for interventional radiology," Proc. 2008 ACM Symp. Virtual Real. Softw. Technol. - VRST '08, p. 105, 2008.

[10] C. Basdogan, C. H. Ho, and M. a. Srinivasan, "Virtual environments for medical training: Graphical and haptic simulation of laparoscopic common bile duct exploration," IEEE/ASME Trans. Mechatronics, vol. 6, no. 3, pp. 269–285, 2001.

[11] V. Luboz, R. Blazewski, D. Gould, and F. Bello, "Real-time guidewire simulation in complex vascular models," Vis. Comput., vol. 25, no. 9, pp. 827–834, 2009.

[12] M. Bergou, M. Wardetzky, S. Robinson, B. Audoly, and E. Grinspun, "Discrete elastic rods," ACM Trans. Graph., vol. 27, no. 3, p. 1, 2008.

[13] W. Tang, P. Lagadec, D. Gould, T. R. Wan, J. Zhai, and T. How, "A realistic elastic rod model for real-time simulation of minimally invasive vascular interventions," Vis. Comput., vol. 26, no. 9, pp. 1157–1165, 2010.

[14] M. Luo, H. Xie, L. Xie, P. Cai, and L. Gu, "A robust and real-time vascular intervention simulation based on Kirchhoff elastic rod," Comput. Med. Imaging Graph., vol. 38, no. 8, pp. 735–743, 2014.

[15] C. Almeder, Hydrodynamic Modelling and Simulation of the Human Arterial Blood Flow, vol. Band 8, no. November 1999. 1999.

[16] X. Wu, J. Allard, and S. Cotin, "Real-time modeling of vascular flow for angiography simulation.," Med. Image Comput. Comput. Assist. Interv., vol. 10, no. Pt 1, pp. 557–565, 2007.

[17] B. Zhu, M. Iwata, R. Haraguchi, T. Ashihara, N. Umetani, T. Igarashi, and K. Nakazawa, "Sketch-based Dynamic Illustration of Fluid Systems," ACM Trans. Graph., vol. 30, no. 6, p. 1, 2011.

[18] B. J., P. G., B. L., and G. G., "Real-time blood circulation and bleeding model for surgical training," IEEE Trans. Biomed. Eng., vol. 60, no. 4, pp. 1013–1022, 2013.

[19] Z. Luo, J. Cai, S. Wang, Q. Zhao, T. M. Peters, and L. Gu, "Magnetic navigation for thoracic aortic stent-graft deployment using ultrasound image guidance.," IEEE Trans. Biomed. Eng., vol. 60, no. 3, pp. 862–71, 2013.

[20] L. Antiga, "Patient-specific modeling of geometry and blood flow in large arteries," Politec. di Milano, 2002.